Research Article

Journal of Environmental Nanotechnology

Evaluation of Activated Biochar from Sustainable *Sterculia foetida* Shells for the Removal of AB 158 Dye

Yennam Rajesh[1*], Neha Gautam[1], Jai Shah[1], Anil Kumar Thandlam[3], Sakshi Gole[1], Pragati Nirgude[1] and Ganesh Dabhade[2]

[1]Department of Chemical Engineering, K K Wagh Institute of Engineering Education & Research, Nashik, MH, TN, India
[2]Department of Applied Science, K K Wagh Institute of Engineering Education & Research, Nashik, MH, India
[3]Department of Petroleum Technology, Aditya University, Surampalem, AP, India
Received: 04.05.2024 Accepted: 19.06.2024 Published: 30.06.2024
*rajeshiitg09@gmail.com

ABSTRACT

The escalating concern over environmental pollution, particularly stemming from industrial effluents like textile dyes, has necessitated the development of sustainable wastewater treatment methods. This study focuses on utilizing agricultural waste, specifically sterculia foetida shells, to synthesize activated carbon for the removal of Acid Blue 158 (AB 158) dye from aqueous solutions. Through a comprehensive investigation, activated carbon samples were produced using various chemical activating agents and characterized using techniques such as BET surface area analysis, Fourier-transform infrared (FT-IR) spectroscopy, and scanning electron microscopy (SEM). Results indicate that the SFS-AC-K-13 adsorbent exhibited superior adsorption performance, with a maximum dye uptake of 388 mg/g and a removal efficiency of 97.89%, respectively. Equilibrium sorption data were analyzed using Langmuir and Freundlich isotherm models, with the Freundlich model demonstrating the best fit (R2=0.9896) to the experimental data. Comparison with literature values confirms the effectiveness of the synthesized adsorbent in AB 158 dye removal. Overall, this research contributes to sustainable wastewater treatment strategies and highlights the potential of agricultural waste-derived activated carbon for textile dye removal applications.

Keywords: Water treatment; *Sterculia foetida* shells; Acid Blue 158; Isotherms; Adsorption.

1. INTRODUCTION

In recent years, the imperative to address environmental pollution, particularly concerning water contamination from industrial effluents like textile dyes, has grown significantly. This has led to increased interest in developing sustainable methods for wastewater treatment. Utilizing agricultural waste to produce activated carbon, known for its ability to capture pollutants from water, has emerged as a promising solution (Thitame *et al.* 2015). Textile dyes, known for their complex chemical structures and persistence in aquatic environments, pose challenges to conventional wastewater treatment methods. Effective adsorbents capable of selectively capturing and removing these dyes are crucial for mitigating environmental harm. Textile dyes present notable health hazards, including skin irritation, respiratory problems, and potential carcinogenic effects linked to their toxic components (Sudarshan *et al.* 2023). Additionally, improper disposal of dye-laden wastewater leads to contamination of water bodies and soils, posing risks to aquatic ecosystems (Lellis *et al.* 2019) and agricultural lands. While regulatory measures aim to restrict hazardous dye usage, ongoing endeavors are essential to develop safer dyeing methods and explore eco-friendly alternatives.

Activated carbon offers a solution due to its high surface area and porosity, providing numerous active sites for dye molecules to adsorb. Utilizing agricultural waste for activated carbon synthesis offers several advantages over traditional methods. Firstly, it provides a sustainable solution to waste disposal by repurposing abundant agricultural byproducts. Various agricultural resources commonly used for the synthesis of activated carbon include coconut shells (Hu *et al.* 1999), wood (Ramirez *et al.* 2017), rice husks (Rahman *et al.* 2012), corn cobs (Tsai *et al.* 1997), sugarcane bagasse (Foo *et al.* 2010), fruit pits and shells (Djilani *et al.* 2015), almond shells, walnut shells. Among agricultural byproducts, *Sterculia foetida* shells offer potential due to their abundance and underutilization.

Sterculia foetida shells, often discarded as waste, contain rich carbon content suitable for conversion into value-added products (Liu *et al.* 2020). Secondly, this approach presents a cost-effective alternative to commercially available activated carbons, which are derived from non-renewable resources and involve significant manufacturing costs. By subjecting these shells to controlled activation processes, their carbon content can be harnessed to create effective adsorbents (Gnanasundaram *et al.* 2017). By using readily available

and renewable precursors, production costs can be reduced, promoting economic viability and scalability.

In the literature, synthesis of activated carbon from *Sterculia foetida* shells was converted with chemical activation. There are several chemical activating reagents are available for creation of pores, such as potassium hydroxide (KOH), sodium hydroxide (NaOH), zinc chloride ($ZnCl_2$), and phosphoric acid (H_3PO_4) play crucial roles (Rajesh *et al.* 2023). KOH and NaOH serve as strong bases, facilitating chemical activation by reacting with the carbonaceous material to create pores within the activated carbon structure, thereby enhancing surface area and adsorption capacity. $ZnCl_2$ acts both as a chemical activating reagent and a dehydrating agent, forming complexes with the carbonaceous material that decompose at high temperatures to generate a well-developed pore structure in the activated carbon (Zhao *et al.* 2022). KOH and H_3PO_4 contribute to the activation process by promoting the formation of pores and enhancing the surface chemistry of the activated carbon (Yakout *et al.* 2016). Each reagent offers distinct advantages, allowing for the customization of activated carbon properties to suit specific wastewater treatment applications, including the removal of dyes from textile industry effluents.

The efficacy of activated carbon synthesized from *Sterculia foetida* shells are used for removing Acid Blue 158 (AB 158) dye merits investigation due to its potential impact on water quality and environmental sustainability. This study aims to elucidate the adsorption behavior of AB 158 dye onto activated carbon from *Sterculia foetida* shells, contributing to sustainable textile dye removal strategies. It investigates the development of activated carbon from *Sterculia foetida* shells using various chemical activating agents, assesses its characteristics (BET surface area analysis, %yield, FT-IR functional groups & SEM, etc.) and ability to remove AB 158 dye, a common textile effluent solution. Through the rigorous experimentation, this study contributes to sustainable wastewater treatment while addressing the challenges of textile industry effluents.

2. MATERIALS AND METHODS

2.1 Materials

Sterculia foetida shells collected from KK Wagh Institute of Engineering Education and Research Campus, Nashik. The chemicals used in this work are AB 158 Dye (M/s Sree Chemidyes, Bangalore, India) H_3PO_4, KOH, NaOH, $ZnCl_2$, HCl and deionised water. All the chemicals were used in analytical grade only. The chemical structure of Acid Blue 158 has shown in Fig. 1. The molecular formula of AB158 dye is $C_{20}H_{11}CrN_2Na_2O_9S_2$ with IUPAC name disodium; chromium (3^+); 3-oxido-4-[(1-oxido-8-sulfonatonaphthalen-2-yl) diazenyl] naphthalene-1-sulfonate; hydroxide.

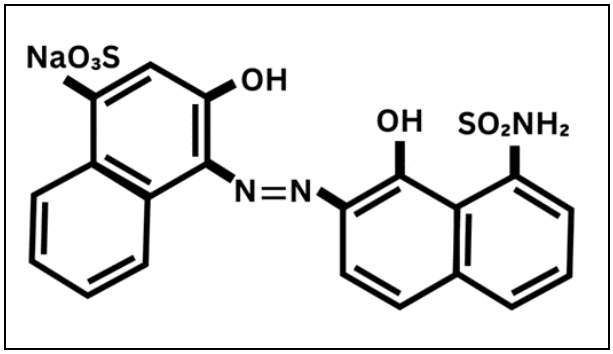

Fig. 1: Chemical Structure of AB 158

2.2 Synthesis of Activated Carbon from sf shells

To initiate the process, *Sterculia foetida* was gathered and thoroughly cleansed with water to eliminate any dust particles. The fruit underwent slicing into pieces and underwent a drying period of 4 hours at 100 °C within an oven. The shells underwent a drying procedure within a hot air oven (Manufacturer: Naval Tech Fabrication) for a duration of 2 to 3 hours at 180 °C to eliminate moisture content. Consequently, the dried shells attained a brittle state. The dried shells were then pulverized using a mixer grinder and subsequently sieved utilizing a sieve shaker (Manufacturer: GLAB India). The resulting powder exhibited particle sizes ranging from 105 to 500 µm.

In prior studies, a range of chemical activating agents has been utilized, including H_3PO_4 (Chakma *et al.* 2016), KOH (Williams *et al.* 2022), NaOH (Cazetta *et al.* 2011), and $ZnCl_2$ (Olivares-Marín *et al.* 2006), respectively. The impregnation ratios of *Sterculia foetida* shell powder to opted chemical activating agents typically vary from 1:1 to 1:3, depending on % yield (Rajesh et al. 2014). Subsequently, the reaction mixture underwent overnight incubation in a hot air oven at 110 °C, followed by carbonization at 300 °C and activation at 500 °C for one hour in a furnace.

The mixture was then neutralized using 0.1 N NaOH and 0.1 N HCl before being dried at 110 °C. Finally, the activated carbon samples were labeled as SFS-K-AC-13, SFS-AC-HP-13, SFS-AC-N-13, and SFS-AC-Z-13 (Chemical activating agents –SFS-AC-K-13) *Sterculia foetida* Activated Carbon) and stored in an air tight container for future experimentation. The summary of the chemical activating agent with respect to % yield was mentioned in Table 1. It represents that among all from the chemical activating agents, potassium hydroxide (KOH) has preferred a great choice due to its yield as 42.1% during activated carbon synthesis.

Table 1. %Yield comparisons for the synthesis of SFS-AC using various chemicals

Sample Name	Impregnation Ratio	Temperature (°C)	Time (min)	% Yield
SFS-AC-N-13	1:3	500	90	45.4
SFS-AC-K-13	1:3	500	90	42.1
SFS-AC-HP-13	1:3	500	90	46.8
SFS-AC-Zn-13	1:3	500	90	53.6

2.3 Batch Adsorption Studies

A stock solution containing 500 mg/L of Acid Blue 158 dye was meticulously prepared by dissolving 50 mg of the dye in 100 mL of distilled water. To ensure consistency and mitigate concentration fluctuations due to various factors, this solution was freshly prepared before each experiment (Mohammed *et al.* 2021). The experimental procedure involved mixing 50 mL of the synthetic dye solution concentration 50-500 mg/L, pH (5-6) and 50 mg of synthesized activated carbon adsorbent powder. This mixture was vigorously agitated for 100 min using an orbital shaker (Model: SESW Orbital). The Orbital shaker operates at 115-120 RPM. Following agitation, the mixture underwent filtration using Whatman filter paper 42 (Model: GE Healthcare and Life Sciences), and Acid Blue 158 present in the filtrate was quantified using a UV-Spectrophotometer (Model: UV-1800 Shimadzu *V Spectrophotometer) at a wavelength of 632 nm. The percentage of dye removal was calculated based on the initial and final concentrations of the dye. Subsequently, the batch adsorption process was employed to analyze the % adsorption and capacity (mg/g) under various conditions, followed by an investigation of adsorption characteristics (Namasivayam *et al.* 1994). To determine the removal percentage, the following equations were utilized:

$$\text{Removal}\,\% = \frac{(C_0 - C_e)}{C_0} \times 100 \quad (1)$$

$$\text{Adsortpion capacity (mg/g)} = \frac{V \times (C_0 - C_e)}{W} \quad (2)$$

Where, C_0 is the initial concentration of Acid Blue 158 in the synthetic solution, in mg/L, C_e is the equilibrium adsorption concentration of Acid Blue 158, in mg/L, W is the adsorbent dosage, in g, V is the volume of the synthetic dye solution, in mL, q_e is the mass of solute adsorbed per mass of adsorbent at equilibrium, in mg/g.

This batch mode experiment facilitated the investigation of the adsorption of Acid Blue 158 onto the SFS-AC-K-13 adsorbent under different optimized conditions like time and enabled the determination of the effectiveness of our adsorbent in removing the dye from the synthetic dye solution.

2.4 Adsorbent Characterization

The final adsorbent (designated as SFS-AC-K-13) underwent characterization through Fourier transform infrared spectrometry (FT-IR) using a Perkin-Elmer PE-RXI instrument and BET Surface Area Analysis conducted with a Beckman Coulter SA-3100 apparatus. Additionally, the determination of BET surface areas and monolayer volumes for SFS-AC-K-13 adsorbents was accomplished using a Beckman Coulter SA-3100 surface area analyzer, employing a nitrogen adsorption isotherm performed at 150 °C. The investigation of various functional groups present in both untreated and treated adsorbents was carried out using FT-IR analysis within the spectral range of 400 – 4000 cm^{-1}. Morphological studies were conducted with Scanning Electron Microscopy (SEM) with a JEOL JSM 6490 LV instrument.

3. RESULTS AND DISCUSSION

3.1 BET Surface Area Analysis

The optimized SFS-AC adsorbents (SFS-K-AC- 13, SFS-AC-N-13, SFS-AC-Z-13, and SFS-AC-HP-13) are prepared by using various chemical activating agents such as H_3PO_4, KOH, NaOH and $ZnCl_2$, respectively. They were tested with BET surface area analysis, and those were shown different porous structures and specific surface areas (Rahman *et al.* 2012). Potassium hydroxide (KOH) has emerged as a preferred choice due to its exceptional ability to create micropores as well as mesopores, thereby enhancing the total pore volume and diameter during SFS-AC synthesis. The adsorbent surface enables the formation of micropores and mesopores due to the occurrence of KOH over the surface of SFS-AC-K-13. A summary of the synthesized SFS-AC adsorbents surface properties were presented in Table 2. It shows that SFS-AC-K-13 is the best adsorbent based on its BET surface area (1225.1 m^2/g) and porous structure (0.7498 cc/g), respectively. Therefore, further studies were carried out with the SFS-AC-K-13 adsorbent, and similar surface properties were reported by (Sudarshan *et al.* 2023).

Table 2. Surface properties of SFS-AC adsorbents using different chemical activating agents

Sample Name	BET Surface Area (m^2/g)	Micro-pore volume (cc/g)	Total pore volume (cc/g)	Average pore diameter (Ao)
SFS-AC-N-13	1138.5	0.350	0.6611	12.150
SFS-AC-K-13	1225.1	0.329	0.7498	11.317
SFS-AC-HP-13	1087.3	0.396	0.4722	13.321
SFS-AC-Zn-13	613.6	0.218	0.326	16.250

3.2 FT-IR Analysis

In our investigation, FT-IR analysis was utilized to characterize both the untreated and treated adsorption of SFS-AC-K-13 adsorbents has reported in Table 3. These delineate a comprehensive analysis of the functional groups present on the adsorbent surface, showcasing the alterations following treatment with KOH, which facilitated the emergence of different functional groups on the surface of the SFS-AC-K-13 adsorbent (Hameed *et al.* 2008).

The FT-IR spectrum of SFS-AC-K-13 exhibits a broad band in the region of 3400 to 3300 cm^{-1} that can be assigned to the O-H stretching vibration of cellulose molecules (Gómez *et al.* 2007). Possible assignment of frequencies of functional group in raw *Sterculia foetida* fruit shell fibre was found at 3390 cm^{-1} as O-H stretching of α-cellulose, 2930 cm^{-1} as C-H stretching, 2858 cm^{-1} as CH2 symmetric stretching (cellulose and hemicelluloses), 1641 cm^{-1} as adsorbed OH water, 896 cm−1 as β-glucosidic linkage, 1037 cm^{-1} as C-O stretch/C-C stretch, 1040–1090 cm^{-1} as antisymmetric stretching modes of the phosphate group, 1037 cm^{-1} and 1249 cm^{-1} as C-O stretching of phenolic compounds (lignin), additional peak at 1604 cm^{-1} as stretching vibration of C=C in aromatic group and potassium peak available at 404 cm^{-1}, respectively. The similar stretching vibrations are reported earlier in the literature as (Manikandan *et al.* 2021).

Table 3. FT-IR analysis of SFS-AC-K-13 adsorbent and Adsorbed SFS-AC-K-13

Wave number (cm^{-1})	Functional Groups (SFS- AC-K-13)	Literature Values (cm^{-1}) (Manikandan *et al.* 2021)
3300 and 3400	O-H	3019
2900 and 2841	C-H	2924 and 2833
1500 and 1600	C=C	1591
1641-1652	OH	1650
1100 and 1000	C-O	1743 and1703
1030 and 1040	C-C	1035
404	K	580

3.3 Morphological Studies of SFS-AC-K-13 Adsorbents

The provided SEM images (Fig. 2) depict (a) SFS-AC-K-13 adsorbents prior to adsorption and (b) SFS-AC-K-13 after adsorption, offering clear insight into the porosity and surface texture of the SFS-AC-K-13 adsorbent material. This implies that the surface structure underwent swelling and expansion due to KOH activation, followed by the creation of active pores on SFS-AC-K-13 surface during the final stages of the sintering process. These images distinctly illustrate that subsequent to adsorption, the pores were saturated with AB 158 dye (Foo *et al.* 2013). Elemental analysis of SFS-AC-K-13 unveiled the following composition: carbon (C) at 74.31%, oxygen (O) at 19.23%, potassium (K) at 0.025%, sodium (Na) at 0.035%, magnesium (Mg) at 0.91%, and calcium (Ca) at 1.05%, respectively (Chakma *et al.* 2011).

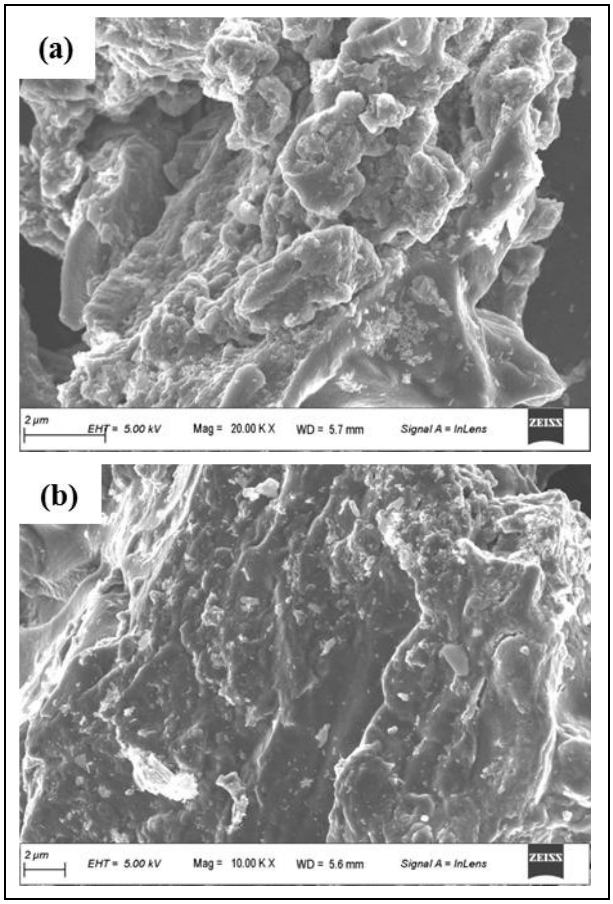

Fig. 2: SEM Analysis of (a) Before adsorption (b) After Adsorption of AB 158 Dye

3.4 Batch Adsorption Studies

The adsorption performance of AB 158 on SFS-AC-K-13 was investigated by using (Manikandan *et al.* 2021), the optimal parameters such as pH (5-6), Dosage (50 mg), time (100 min), and Concentration (50-500 mg/L), respectively. Fig. 3 represents the variations of adsorption capacity and % removal of AB 158 on SFS-AC-K-13 adsorbent. The variation in concentrations of AB 158 dye solution from 50 to 500 mg/L, highest adsorption capacity was obtained as 388 mg/g and % removal as 97.89, respectively. In comparison with literature, modified SFS-AC prepared with H_3PO_4 as shown better adsorption capacity of 370 mg/g and % removal 96 for methylene blue dye. Thus, the prepared SFS-AC adsorbent was effective for AB 158 dye adsorption from synthetic dye solutions. The adsorption capacity increased with an increase in dye concentrations due to more availability of acid blue dye ions over the surface of SFS-AC-K-13. A comparison of adsorption capacity for other adsorbents from literature confirms

that only SFS-AC-K-13 shown higher values of adsorption capacity (Herrera-González *et al.* 2019).

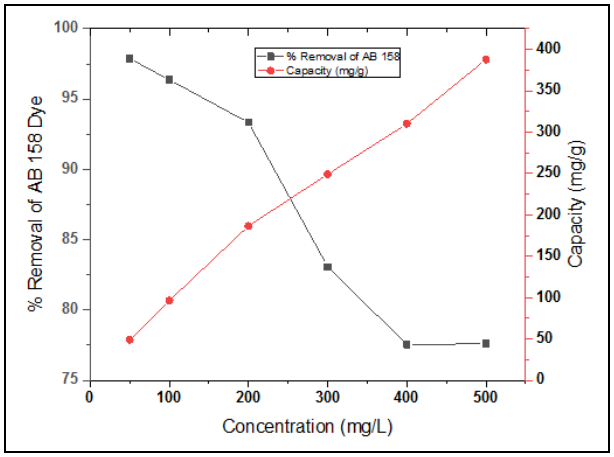

Fig. 3: Adsorption characteristics of AB 158 on SFS-AC-K-13 adsorbent

3.5 Equilibrium Isotherms

For the efficient design of sorption systems, analyzing equilibrium sorption data is essential. The interaction between the adsorbed species and the adsorbent surface dictates the adsorption process, involving Van der Waals forces, hydrophobic forces, chemical bonds, and hydrogen bonds (Ramesh et al., 2008). Adsorption isotherms elucidate the relationship between the amount of solute absorbed per unit weight of solid adsorbent and the remaining amount in the solution at equilibrium. The Langmuir and Freundlich isotherm models are commonly used to elucidate the adsorption of AB 158 dye adsorption on SFS-AC adsorbents. Both models are applied to interpret the equilibrium data of adsorbents, suggesting either monolayer or multilayer adsorption depending on the adsorbent surface type (Rajesh *et al.* 2023).

The Freundlich isotherm proposes that dye adsorption occurs as a heterogeneous process on the adsorbent surface, contrasting with the Langmuir model, which predicts sorption on the homogeneous surface of the adsorbent, forming a saturation monolayer. Additionally, the Temkin and Redlich models serve as reliable representations of adsorption equilibrium. In this study, the suitability of each of the four models in accurately depicting the experimentally observed adsorption properties of SFS-AC adsorbents was evaluated. However, the Temkin and Redlich-Peterson models exhibited poor fit to the isothermal data (Derle *et al.* 2023). Consequently, the author included the data from the Langmuir and Freundlich models in the subsequent sections.

Assuming complete monolayer coverage on a homogeneous adsorbent surface without any interaction between the adsorbed ions, the Langmuir equilibrium isotherm model is represented as (Sivaranjanee *et al.* 2022):

$$\frac{C_e}{q_e} = \frac{1}{bq_{max}} + \frac{1}{q_{max}} C_e \qquad (3)$$

Where, C_e is the equilibrium adsorption concentration of AB 158 dye in mg/L, q_e is the mass of solute adsorbed per mass of adsorbent at equilibrium in mg/g, q_{max} is the Langmuir monolayer capacity in mg/g, b is the Langmuir equilibrium constant; and C_0 is the initial concentration of AB 158 dye in aqueous solution in mg/L.

The Freundlich isotherm model is defined as follows, assuming the exponential distribution of active centers, heterogeneous surface, and infinite surface coverage (Babatunde *et al.* 2022):

$$\log q_e = \log K_f + m \log C_e \qquad (4)$$

Where, K_f is the Freundlich isotherm coefficient, m is the amount of adsorbent taken in mg/L.

The concentration study was conducted prior to isotherm modeling, utilizing the Langmuir and Freundlich isotherm models, respectively, for AB 158 dye adsorption on SFS-AC-K-13 using synthetic dye solutions (Rajesh *et al.* 2023). The suitability of the Langmuir and Freundlich isotherms for AB 158 dye adsorption characteristics is depicted in Figs. 4 and 5. Both models demonstrated a good fit to the measured equilibrium adsorption data. However, the Freundlich isotherm exhibited the highest fitness (R^2 = 0.9896) for AB 158 dye adsorption, suggesting that heterogeneous adsorption is the predominant mechanism during AB 158 dye adsorption, involving functional groups containing O–H stretching of α-cellulose and C–H stretching. Additionally, the confirmation that the 1/n value consistently falls between 0 and 1 indicates that the chosen adsorbent-adsorbate system is favorable for AB 158 dye removal (Kuoppamäki *et al.* 2019).

The findings of this study demonstrate a performance comparable to other activated carbons, as listed in Table 4. They suggest that the activation method or material utilized in this study is more effective in removing dyes, and the adsorption capacities of various precursor-activated carbons. Importantly, the evaluated dye adsorption capacity values align with those observed for aqueous solutions using activated carbon adsorbents (Kumar *et al.* 2012). However, higher adsorption capacity is achieved only for modified SFS-AC adsorbents, attributed to the enhanced adsorption characteristics resulting from various chemical activating agents. This comparative analysis facilitates a straightforward evaluation of SFS-AC-K-13 performance, which proves competitive with literature values for the removal of dyes (Shaikhiev *et al.* 2021).

Table 4. A summary of AC Adsorption Capacities and %Removal for various dyes

Adsorbent Name	Dye	Capacity (mg/g)	Removal (%)	Reference
SFS-AC	Acid Blue 158	388	98.6	Present Work
Almond Shells	Methylene Blue	329	96.0	(Mohammed *et al.* 2021)
Almond Shells	Crystal Violet	376	91.7	(Boulika *et al.* 2022)
Coir Pith-AC	Methylene Blue	218	96.0	(Thitame *et al.* 2015)

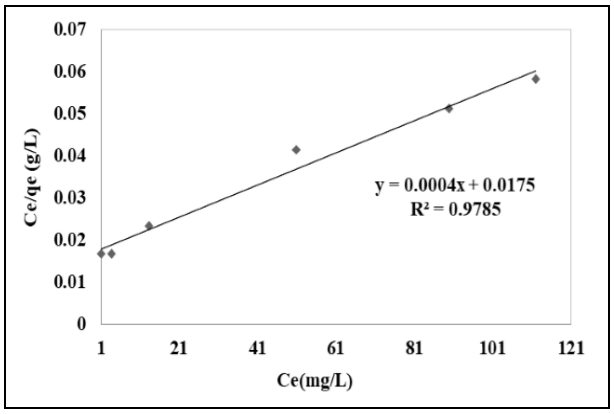

Fig. 4: Fitness of Langmuir Isotherms Model for AB 158 on SFS-AC-K-13 adsorbent

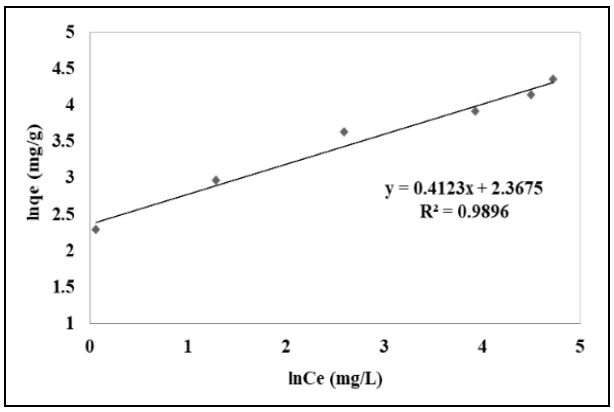

Fig. 5: Fitness of Freundlich Isotherms Model for AB 158 on SFS-AC-K-13 adsorbent

4. CONCLUSION

This study demonstrates the potential of *Sterculia foetida* shells as a sustainable precursor for producing activated carbon to remove Acid Blue 158 (AB 158) dye from wastewater. By synthesizing the activated carbon samples using various chemical activating agents, including KOH, NaOH, $ZnCl_2$, and H_3PO_4, respectively. The authors identified the SFS-AC-K-13 adsorbent as highly effective based on detailed characterization, including its BET surface area (12255.1 m^2/g), its availability of functional groups (OH, C-O, C-C, and K), and its porous structure surface. Batch adsorption experiments revealed that SFS-AC-K-13 achieved a maximum adsorption capacity of 388 mg/g and a removal efficiency of 97.89% at a concentration of 50-500 mg/L, respectively. The Langmuir and Freundlich models provided good fitness for equilibrium sorption data, and it indicates the Freundlich model was the best fit for experimental data. And also suggesting that heterogeneous adsorption is the primary mechanism during AB 158 dye adsorption. This work shows the pathway for producing activated carbon from tree waste materials and applications towards separation of various pollutants from wastewater.

ACKNOWLEDGEMENT

The authors would like to thank the Management of K.K.Wagh Institute of Engineering Education and Research, Nashik (Affiliated to Savitribai Phule Pune University) for providing the laboratory and infrastructural facilities and support. Also, the authors are thankful to the management of ICSPT team and special thanks to Dr. J. Anand Kumar, Associate Professor, and NIT Raipur for his constant support and providing us the opportunity to publish our research work in the scientific community.

FUNDING

This research received no specific grant from any funding agency in the public, commercial, or not-for-profit sectors.

CONFLICTS OF INTEREST

The authors declare that there is no conflict of interest.

COPYRIGHT

REFERENCES

Babatunde, K. A., Negash, B. M., Jufar, S. R., Ahmed, T. Y., Mojid, M. R., Adsorption of gases on heterogeneous shale surfaces: A review, *J. Pet. Sci. Eng.* 208, 109466 (2022). https://doi.org/10.1016/j.petrol.2021.109466

Boulika, H., El Hajam, M., Hajji Nabih, M., Idrissi Kandri, N., Zerouale, A., Activated carbon from almond shells using an eco-compatible method: screening, optimization, characterization, and adsorption performance testing, *RSC Adv.* 12(53), 34393–34403 (2022). https://doi.org/10.1039/D2RA06220H

Cazetta, A. L., Vargas, A. M. M., Nogami, E. M., Kunita, M. H., Guilherme, M. R., Martins, A. C., Silva, T. L., Moraes, J. C. G., Almeida, V. C., NaOH-activated carbon of high surface area produced from coconut shell: Kinetics and equilibrium studies from the methylene blue adsorption, *Chem. Eng. J.* 174(1), 117–125 (2011). https://doi.org/10.1016/j.cej.2011.08.058

Chakma, S., Moholkar, V. S., Synthesis of bi-metallic oxides nanotubes for fast removal of dye using adsorption and sonocatalysis process, *J. Ind. Eng. Chem.* 37, 84–89 (2016). https://doi.org/10.1016/j.jiec.2016.03.009

Chakma, S., Moholkar, V. S., Mechanistic features of ultrasonic desorption of aromatic pollutants, *Chem. Eng. J.* 175, 356–367 (2011). https://doi.org/10.1016/j.cej.2011.09.123

Derle, S. N., Parikh, P. A., Parikh, J. K., Jain, S. N., Caustic soda treated dried foliage of Arachis hypogaea as a promising biosorbent for Chromacyl Blue GG dye removal, Biomass Convers Biorefinery (2023). https://doi.org/10.1007/s13399-023-04898-z

Djilani, C., Zaghdoudi, R., Djazi, F., Bouchekima, B., Lallam, A., Modarressi, A., Rogalski, M., Adsorption of dyes on activated carbon prepared from apricot stones and commercial activated carbon, *J. Taiwan Inst. Chem. Eng.* 53, 112–121 (2015). https://doi.org/10.1016/j.jtice.2015.02.025

Foo, K. Y., Hameed, B. H., An overview of dye removal via activated carbon adsorption process, *Desalin. Water Treat.* 19(1–3), 255–274 (2010). https://doi.org/10.5004/dwt.2010.1214

Foo, K. Y., Lee, L. K., Hameed, B. H., Preparation of activated carbon from sugarcane bagasse by microwave assisted activation for the remediation of semi-aerobic landfill leachate, *Bioresour. Technol.* 134, 166–172 (2013). https://doi.org/10.1016/j.biortech.2013.01.139

Gnanasundaram, N., Loganathan, M., Singh, A., Optimization and Performance parameters for adsorption of Cr 6+ by microwave assisted carbon from *Sterculia foetida* shells, *IOP Conf. Ser. Mater. Sci. Eng.* 206, 012065 (2017). https://doi.org/10.1088/1757-899X/206/1/012065

Gómez, V., Larrechi, M. S., Callao, M. P., Kinetic and adsorption study of acid dye removal using activated carbon, *Chemosphere* 69(7), 1151–1158 (2007). https://doi.org/10.1016/j.chemosphere.2007.03.076

Hameed, B. H., Tan, I. A. W., Ahmad, A. L., Optimization of basic dye removal by oil palm fibre-based activated carbon using response surface methodology, *J. Hazard. Mater.* 158(2–3), 324–332 (2008). https://doi.org/10.1016/j.jhazmat.2008.01.088

Herrera-González, A. M., Caldera-Villalobos, M., Peláez-Cid, A.-A., Adsorption of textile dyes using an activated carbon and crosslinked polyvinyl phosphonic acid composite, *J. Environ. Manage.* 234, 237–244 (2019). https://doi.org/10.1016/j.jenvman.2019.01.012

Hu, Z., Srinivasan, M. ., Preparation of high-surface-area activated carbons from coconut shell, *Microporous Mesoporous Mater.* 27(1), 11–18 (1999). https://doi.org/10.1016/S1387-1811(98)00183-8

Kumar, P., Agnihotri, R., Wasewar, K. L., Uslu, H., Yoo, C., Status of adsorptive removal of dye from textile industry effluent, *Desalin. Water Treat.* 50(1–3), 226–244 (2012). https://doi.org/10.1080/19443994.2012.719472

Kuoppamäki, K., Hagner, M., Valtanen, M., Setälä, H., Using biochar to purify runoff in road verges of urbanised watersheds: A large-scale field lysimeter study, *Watershed Ecol. Environ.* 1, 15–25 (2019). https://doi.org/10.1016/j.wsee.2019.05.001

Lellis, B., Fávaro-Polonio, C. Z., Pamphile, J. A., Polonio, J. C., Effects of textile dyes on health and the environment and bioremediation potential of living organisms, *Biotechnol. Res. Innov.* 3(2), 275–290 (2019). https://doi.org/10.1016/j.biori.2019.09.001

Liu, R., Xiao, H., Pang, S. D., Geng, J., Yang, H., Application of *Sterculia foetida* petiole wastes in lightweight pervious concrete, *J. Clean. Prod.* 246, 118972 (2020). https://doi.org/10.1016/j.jclepro.2019.118972

Manikandan, G., Meyyappan, N., Pitchai, R., -Removal Of Basic Green 4 Dye Using Raw and Surface Modified Streculia Foetida Seeds, Res Sq. (2021). https://doi.org/https://doi.org/10.21203/rs.3.rs-179380/v1

Mohammed, E. K., Noureddine, El Messaoudi Abdellah, D., Safae, B., Abdellah, L., Zahra Goodarzvand, C., Iqbal, M., Organic Dyes Adsorption on the Almond Shell (Prunus dulcis) as Agricultural Solid Waste from Aqueous Solution in Single and Binary Mixture Systems, *Biointerface Res. Appl. Chem.* 12(2), 2022–2040 (2021). https://doi.org/10.33263/BRIAC122.20222040

Namasivayam, C., Jeyakumar, R., Yamuna, R. T., Dye removal from wastewater by adsorption on 'waste' Fe(III)/Cr(III) hydroxide, *Waste Manag.* 14(7), 643–648 (1994). https://doi.org/10.1016/0956-053X(94)90036-1

Olivares-Marín, M., Fernández-González, C., Macías-García, A., Gómez-Serrano, V., Preparation of activated carbon from cherry stones by chemical activation with ZnCl2, *Appl. Surf. Sci.* 252(17), 5967–5971 (2006). https://doi.org/10.1016/j.apsusc.2005.11.008

Rahman, M. A., Amin, S. M. R., Alam, A. M. S., Removal of Methylene Blue from Waste Water Using Activated Carbon Prepared from Rice Husk, *Dhaka Univ. J. Sci.* 60(2), 185–189 (2012). https://doi.org/10.3329/dujs.v60i2.11491

Rajesh, Y., Boricha, H., Suryavanshi, A., Gajare, A., Jain, S., Suresh, K., Synthesis, characterization and adsorption studies on activated carbon adsorbent synthesized from Kigelia africana for removal of acid blue 113 dye from synthetic solution, Mater Today Proc. (2023). https://doi.org/10.1016/j.matpr.2023.11.046

Ramirez, A. P., Giraldo, S., Ulloa, M., Flórez, E., Acelas, N. Y., Production and characterization of activated carbon from wood wastes, *J. Phys. Conf. Ser.* 935, 012012 (2017). https://doi.org/10.1088/1742-6596/935/1/012012

Shaikhiev, I. G., Kraysman, N. V., Sverguzova, S. V., Review of Almond (Prunus Dulcis) Shell Use to Remove Pollutants from Aquatic Environments, *Biointerface Res. Appl. Chem.* 11(6), 14866–14880 (2021). https://doi.org/10.33263/BRIAC116.1486614880

Sivaranjanee, R., Kumar, P. S., Mahalaxmi, S., A review on agro-based materials on the separation of environmental pollutants from water system, *Chem. Eng. Res. Des.* 181, 423–457 (2022). https://doi.org/10.1016/j.cherd.2022.04.002

Sudarshan, S., Harikrishnan, S., RathiBhuvaneswari, G., Alamelu, V., Aanand, S., Rajasekar, A., Govarthanan, M., Impact of textile dyes on human health and bioremediation of textile industry effluent using microorganisms: current status and future prospects, J Appl Microbiol., 134(2), (2023). https://doi.org/10.1093/jambio/lxac064

Thitame, P. V., Shukla, S. R., Porosity Development of Activated Carbons Prepared from Wild Almond Shells and Coir Pith Using Phosphoric Acid, *Chem. Eng. Commun.* , 00986445.2015.1104503 (2015). https://doi.org/10.1080/00986445.2015.1104503

Tsai, W. T., Chang, C. Y., Lee, S. L., Preparation and characterization of activated carbons from corn cob, *Carbon N. Y.* 35(8), 1198–1200 (1997). https://doi.org/10.1016/S0008-6223(97)84654-4

Williams, N. E., Oba, O. A., Aydinlik, N. P., Modification, Production, and Methods of KOH-Activated Carbon, *ChemBioEng Rev.* 9(2), 164–189 (2022). https://doi.org/10.1002/cben.202100030

Yakout, S. M., Sharaf El-Deen, G., Characterization of activated carbon prepared by phosphoric acid activation of olive stones, *Arab. J. Chem.* 9, S1155–S1162 (2016). https://doi.org/10.1016/j.arabjc.2011.12.002

Zhao, H., Zhong, H., Jiang, Y., Li, H., Tang, P., Li, D., Feng, Y., Porous ZnCl2-Activated Carbon from Shaddock Peel: Methylene Blue Adsorption Behavior, *Materials (Basel).* 15(3), 895 (2022). https://doi.org/10.3390/ma15030895